

---

## *CHAPTER 6: Classification of Magnetic Spin Freezing of $\text{Ho}_2\text{Ti}_2\text{O}_7$ and $\text{Dy}_2\text{Ti}_2\text{O}_7$ in Terms of Quantum Criticality*

---

### **6.1 Introduction**

In chapter 5, effect of structural distortions and magnetic perturbation on the spin dynamic of  $\text{Dy}_2\text{Ti}_2\text{O}_7$  has been studied. It has been found that the Ising spin are strongly correlated and sensitive to the nature of neighboring magnetic ion's spins. In these materials, order of dipolar and exchange spin interactions are very small [48], [127]. Because of thermal/quantum fluctuations the rare earth ion's spin fluctuates via local transformation. These fluctuations force these correlated Ising spins to retain a liquid-like disordered phase even at low temperatures [16], [17], [22], [23], [65], [71]. As discussed in chapter 1, these materials possess two spin freezing at  $\sim 16$  K ( $T_f$ ) and  $\sim 4$  K ( $T_{ice}$ ) [61], [65], [69], [70]. It has been found that both  $T_f$  and  $T_{ice}$  strongly depend on the strength of the applied magnetic field. Further, spin ice freezing ( $T_{ice}$ ) vanishes above an applied field of 1 T for both DTO and HTO [41], [57], [70]. Furthermore, in HTO spin dynamics are governed by the quantum fluctuation up to 30 K whereas in case of DTO it existed only up to  $\sim 12$  K [61], [71]. The dependency of spin freezing on magnetic field and involvement of possible quantum fluctuations, DTO and HTO can be investigated in terms of "quantum criticality" of Quantum Phase Transitions (QPT). QPT follows the  $(x-x_C)^{1/2}$  behavior with non-thermal parameters whereas in the classical region it follows  $(x-x_C)$  type variation [76]–[78]. Through the application of non-thermal control variables, such as pressure (P), composition(x), or magnetic field (H), one can obtain the Quantum Critical Point (QCP) as well as the region of quantum criticality of the materials. The discernment of quantum criticality and its associated

exotic phases in magnetically frustrated materials are one of the important problems of physics as well as from the application point of view [140], [141]. In this chapter, classification of the quantum critical region and control variables which affects the quantum critical point of HTO and DTO has been investigated.

## **6.2 Results and discussion**

### **6.2.1 Magnetic analysis of $\text{Ho}_2\text{Ti}_2\text{O}_7$ and $\text{Dy}_2\text{Ti}_2\text{O}_7$**

#### **6.2.1.1 ac susceptibility and H-T Phase diagram of $\text{Ho}_2\text{Ti}_2\text{O}_7$**

Figure 6.1 shows the temperature dependence of the real part ( $\chi'$ ) of the ac susceptibility under different dc bias magnetic field in the range of 0 to 6 T measured at 500 Hz. For the sake of clarity, the field-dependent data has been split into two parts. Figure 6.1 (a) shows the ac susceptibility response up to an applied field of 1 T. The inset of figure 6.1 (a) shows the changes in the freezing temperature more clearly. It has been found that in absence of field, no freezing is observed up to lowest measured temperature as shown in figure 6.1(a). On application of 0.35 T of external field, freezing belonging to  $T_{\text{ice}}$  appeared prominently, whereas the freezing corresponding to  $T_f$  has yet to develop. On further increase in the magnetic field i.e. 0.5 T, both freezing correspondings to  $T_f$  and  $T_{\text{ice}}$  are distinctly observed. On further increase in the applied magnetic field, the  $T_{\text{ice}}$  freezing gets suppressed whereas  $T_f$  freezing becomes pronounced and gradually shifted towards the higher temperature side.

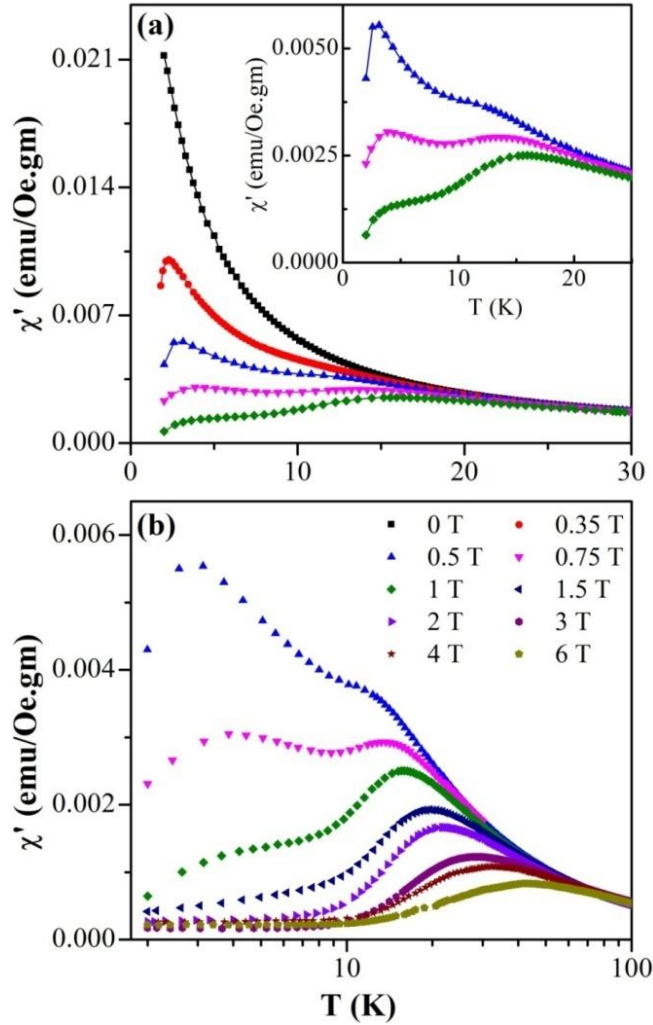


*Figure 6.1: Temperature dependence of the real part of ac susceptibility measured at 500 Hz for dc bias field; (a) 0, 0.35, 0.5, 0.75 and 1 T and (b) 0.5, 0.75, 1, 1.5, 2, 3, 4 and 6 T for  $\text{Ho}_2\text{Ti}_2\text{O}_7$  compound.*

With the help of the obtained values of  $T_f$  with respect to  $H$ ,  $T_f$  vs.  $H$  plot has been shown in figure 6.2 (a). As discussed above, in the quantum critical region,  $T_f$  follows  $(H-H_C)^{1/2}$  variation whereas in the classical region it obeys a linear relation [76], [142], [143]. To investigate the type of dependency of  $T_f$  on  $H$ , observed  $T_f$  vs.  $H$  plot is fitted using  $(H-H_C)^{1/2}$  expression in the field range 0.5-2 T and extrapolated. The value of the critical field ( $H_C$ ) at QCP has been found  $340 \pm 35$  Oe. The fitted curve is extrapolated up to 0 T to 7 T and shown by the pink color solid line in  $T_f$  vs.  $H$  plot (figure 6.2 (a)). The so obtained phase diagram

shows the deviation of  $T_f$  from  $(H-H_C)^{1/2}$  variation at higher field. To obtain the deviation temperature, a linear fit has been performed in 3-6 T field range and extrapolated at the lower field (red line). The extrapolated curve shows a clear deviation from the linear behavior in the lower field region. The point of intersection of both fitted curve shows the crossover region at  $\sim 28.5$  K temperature.

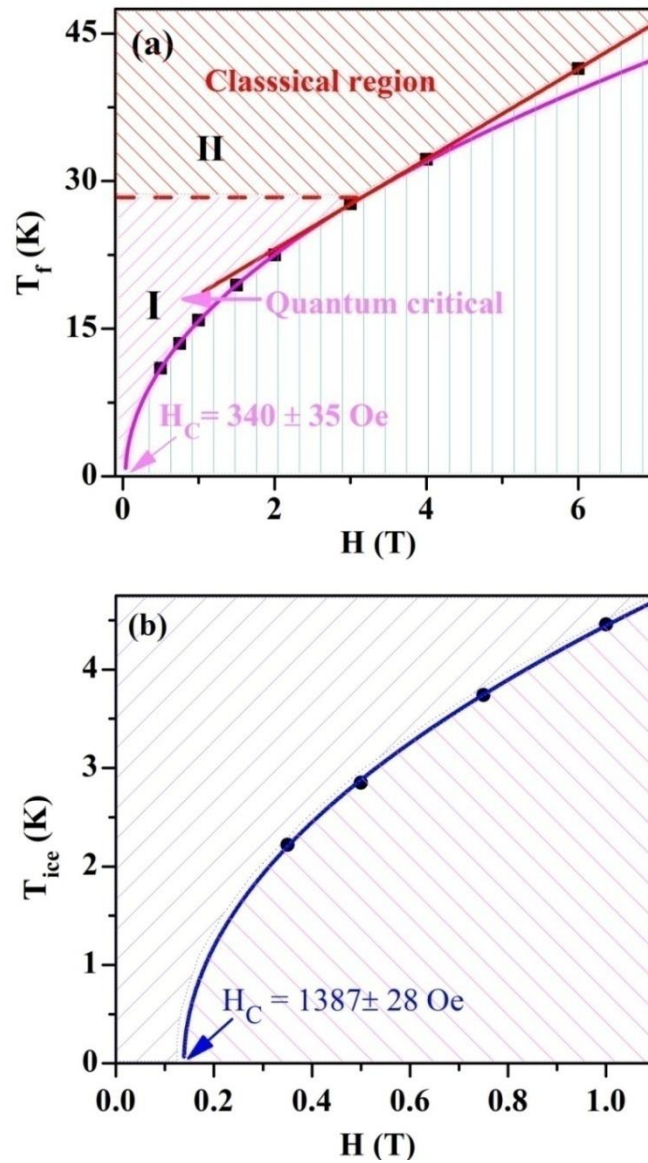


Figure 6.2:  $H$ - $T$  phase diagram of the  $\text{Ho}_2\text{Ti}_2\text{O}_7$  compound for (a)  $T_f$  and (b)  $T_{ice}$  freezing with deduced value of  $H_C$ . The  $(H-H_C)^{1/2}$  fit is represented by solid pink and blue line whereas the linear fit is represented by a solid red line.

On the basis of observed fitting, H-T phase diagram is categorized into two distinct regions termed as-quantum critical and classical represented by I and II in the figure 6.2 (a). In regime I existed upto ~28.5 K,  $T_f$  vs. H plot follows  $(H-H_C)^{1/2}$  relation. Above 28.5 K, (regime II), a crossover from quantum critical to classical region takes place, where spin dynamics is governed by classical thermal fluctuations. It has been noted that observed crossover temperature is almost same as obtained from neutron scattering measurement for this compound, thus further confirming the validity of the H-T phase diagram [70]–[72].

These experiments suggest that effect of magnetic field on  $T_{ice}$  is more prominent in comparison to single ion spin freezing  $T_f$ . M. Vojta has shown that, for these frustrated materials, there is a possibility that spin ice freezing may affect the value of the critical field at QCP [140]. For the spin ice freezing,  $T_{ice}$  vs. H plot is shown in figure 6.2 (b). The  $(H-H_C)^{1/2}$  fitting yield critical field,  $H_C = 1387 \pm 28$  Oe at QCP which is larger than the critical field obtained for that of the single ion spin freezing (340Oe). The  $(H-H_C)^{1/2}$ -type variation of  $T_{ice}$  further confirms the formation of this exotic state in the quantum critical region.

### **6.2.1.2 ac susceptibility and H-T Phase diagram of Dy<sub>2</sub>Ti<sub>2</sub>O<sub>7</sub>**

To further confirm the validity of the H-T phase diagram, ac susceptibility measurement at different magnetic field has been performed on DTO as well. In the case of DTO, quantum fluctuations existed up to 12 K [61], [65]. This means that observed single spin freezing temperature (~16 K) will show the classical linear relation in H- $T_f$  plot whereas lower temperature spin ice freezing shows  $(H-H_C)^{1/2}$ -type variation. Figure 6.3 shows the temperature dependence of the real part of ac susceptibility of DTO measured at 200 Hz frequency for different magnetic field. Unlike to HTO, in this compound, both  $T_f$  and  $T_{ice}$  freezing is observed in absence of an external magnetic field. However, on the application of

magnetic field, both freezing gradually shifted towards the higher temperature similar to HTO.

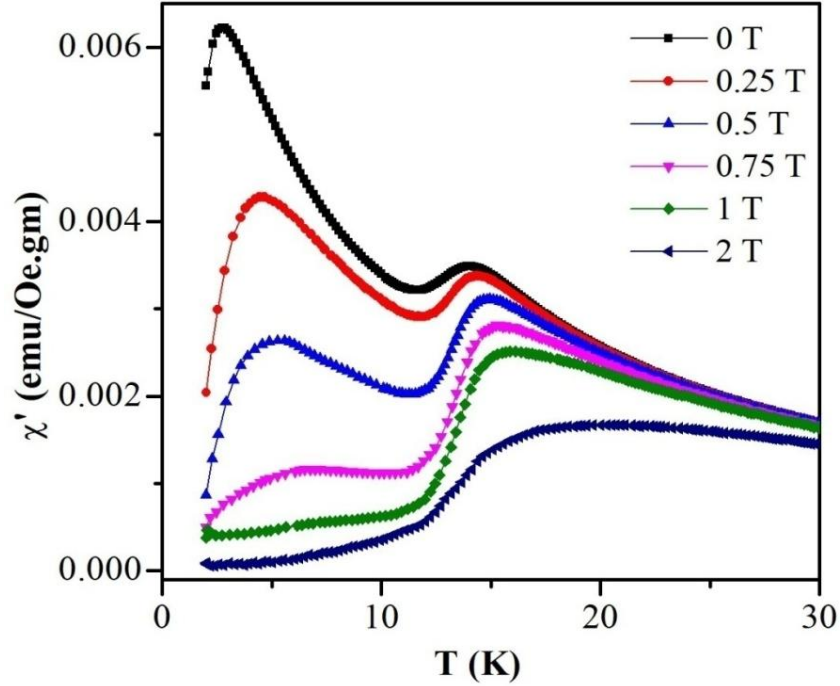


*Figure 6. 3: Real part of magnetic susceptibility of  $\text{Dy}_2\text{Ti}_2\text{O}_7$  compound measured at 200 Hz frequency for 0, 0.25, 0.5, 0.75, 1 and 2 T, dc bias magnetic field.*

With the help of obtained values of  $T_f$  and  $T_{ice}$  with respect to  $H$ ,  $H$ - $T$  phase diagram for both freezings has been plotted and shown in figure 6.4. A linear fit for  $T_f$  vs.  $H$  plot is shown by red color in figure 6.4 (a) thus depicting the classical linear relation. A similar variation in the  $T_f$  with  $H$  has been obtained by shi et al. in ac susceptibility studies of the single crystal of DTO [144]. The linear variation of  $T_f$  with respect to field confirming the classical nature of observed freezing. On the other hand, variation of  $T_{ice}$  freezing with magnetic field shows the  $(H-H_C)^{1/2}$  variation having QCP at  $H_C = -1558 \pm 48$  Oe. The  $(H-H_C)^{1/2}$  variation of spin ice freezing confirms that this freezing lies in the quantum critical region.

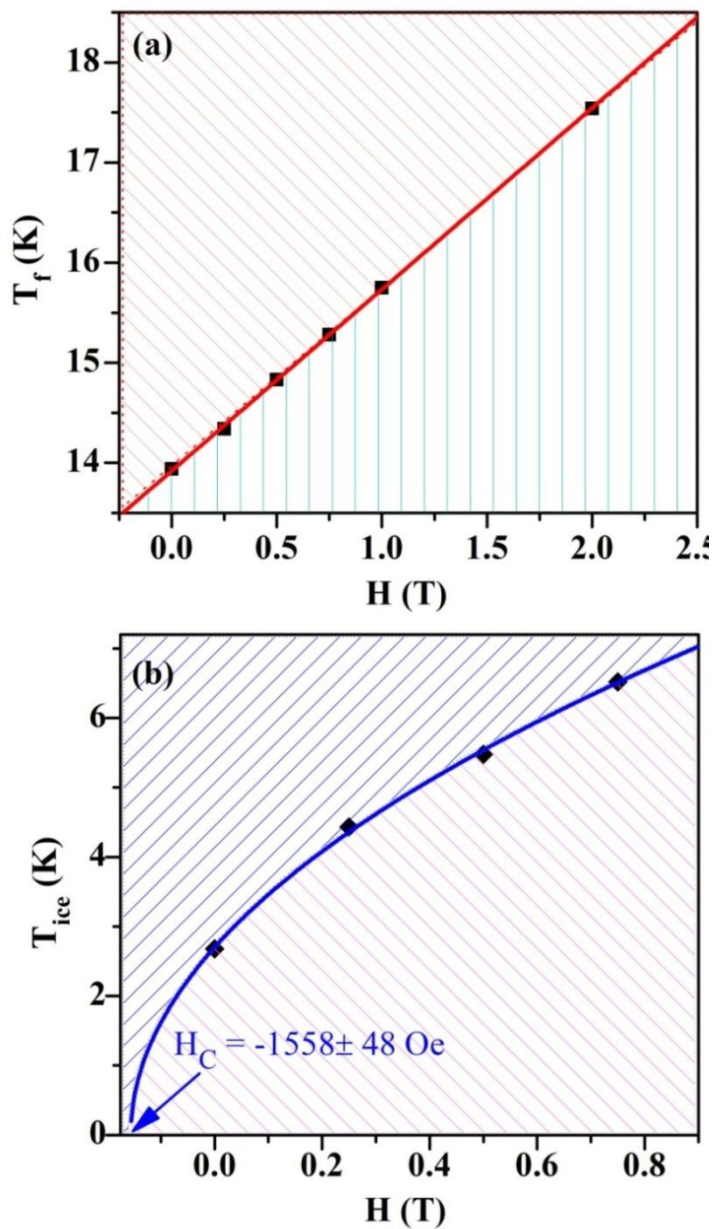


*Figure 6.4: H-T phase diagram of  $\text{Dy}_2\text{Ti}_2\text{O}_7$  compound for (a)  $T_f$  and (b)  $T_{\text{ice}}$  freezing with deduced value of  $H_C$ .*

The negative value of critical field suggests that this compound have very large energy barrier to flip the Ising spin from one direction to another. This energy barrier associated with the local internal magnetic field ( $H_{\text{int}}$ ) induced by crystal field, spin-lattice and magnetic interactions and have exponential relationship with spin flip time. On application of external

perturbation (magnetic field in this case), this underlying energy barrier increases linearly. As the spin-flip time, follows the Arrhenius like behaviour, it increases exponentially, which in turn reflected through emergence and shifting in freezing temperature. This means that positive or negative value of critical field represents the magnitude of the magnetic field needed to obtain the spin freezing at absolute zero temperature via enhancement or suppression in the internal field-induced energy barrier through external variables giving an important physical parameter to control the quantum critical limits.

In the case of HTO, it has been found that  $T_{ice}$  freezing have a larger value of critical field than the  $T_f$  freezing. The increment in the critical field of  $T_{ice}$  freezing indicates that underlying magnetic interaction responsible for this freezing also affecting the energy barrier similar to the magnetic field. To see the effect of magnetic interaction on energy barrier, B-site Mn substituted Ho<sub>2</sub>Ti<sub>1.9</sub>Mn<sub>0.1</sub>O<sub>7</sub> and Dy<sub>2</sub>Ti<sub>1.9</sub>Mn<sub>0.1</sub>O<sub>7</sub> samples have been synthesized. Due to strongly interacting nature of magnetic Mn ion, it is supposed that this substitution will alter the internal field induced energy barrier.

### **6.2.2 Structural analysis of Ho<sub>2</sub>Ti<sub>1.9</sub>Mn<sub>0.1</sub>O<sub>7</sub> and Dy<sub>2</sub>Ti<sub>1.9</sub>Mn<sub>0.1</sub>O<sub>7</sub>**

The diffraction pattern shown in the figure 2.2 and 2.3 in chapter 2 has been analyzed using Rietveld refinement. Through the Rietveld refinement,  $Fd\bar{3}m$  space group and site occupancy of Ho, Dy and Ti/Mn ions at 16c and 16d sites of HTMO and DTMO samples have been confirmed. The obtained fit is remarkably good and shown in figure 6.5. The obtained reliable fitting parameters  $R_p$ ,  $R_{wp}$ ,  $R_{exp}$  and lattice constant are shown in the table 6.1. It has been found that in HTMO and DTMO a decrease in the lattice constant takes place without affecting the cubic  $Fd\bar{3}m$  crystallographic phase.

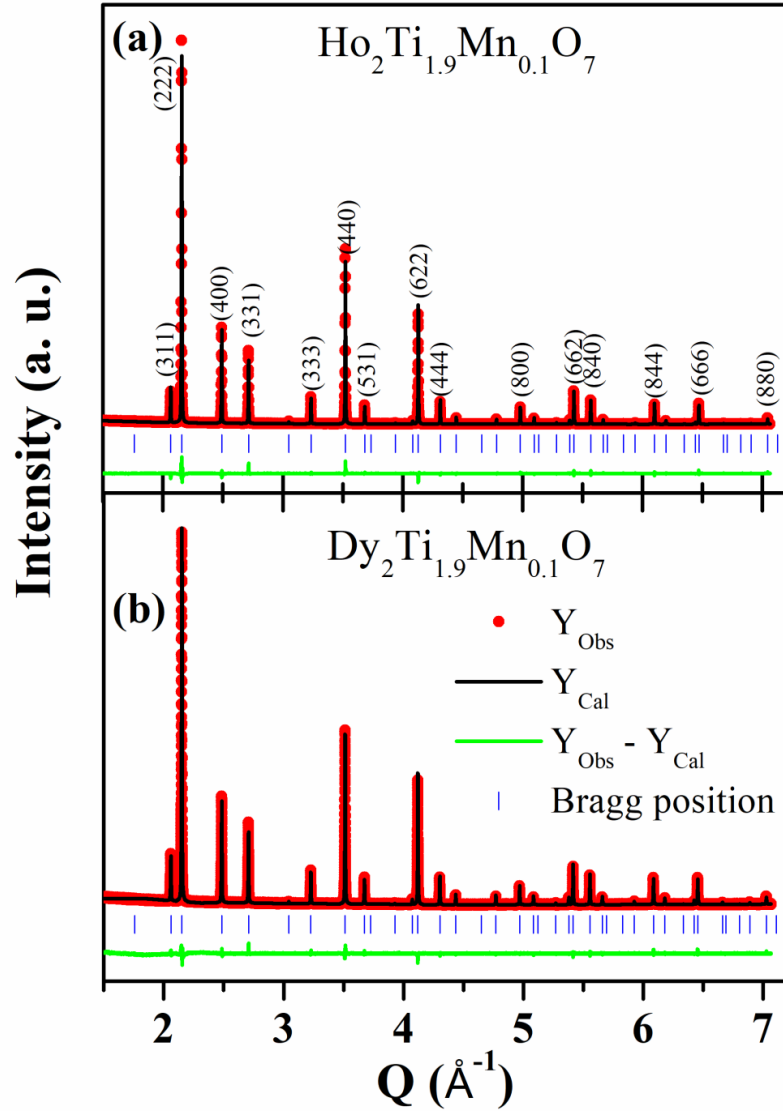


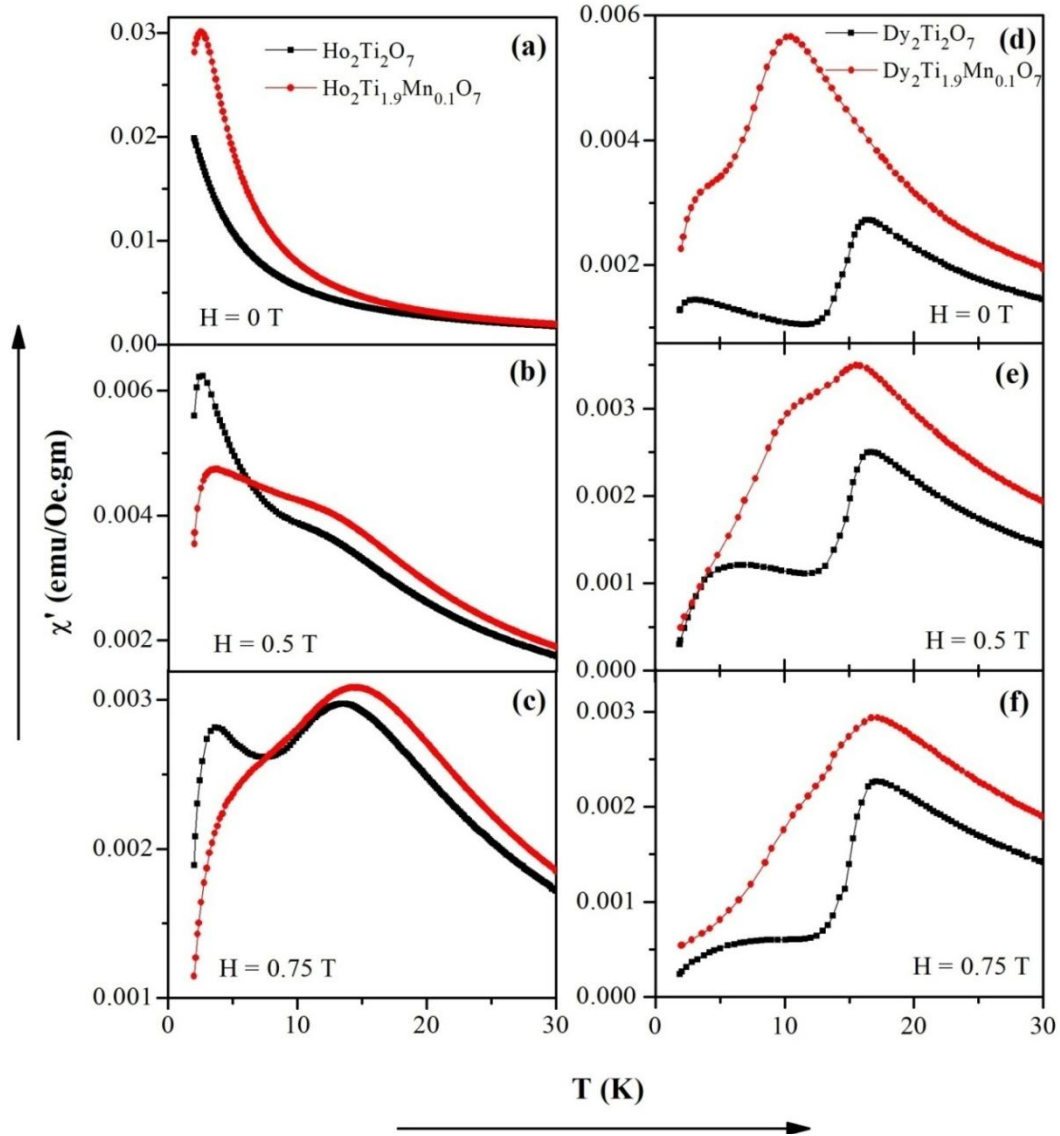
Figure 6.5: Rietveld refinement of x-ray diffraction pattern of polycrystalline; (a)  $\text{Ho}_2\text{Ti}_{1.9}\text{Mn}_{0.1}\text{O}_7$ , and (b)  $\text{Dy}_2\text{Ti}_{1.9}\text{Mn}_{0.1}\text{O}_7$ .

Table 6.1: Details of refinement as obtained from high-resolution x-ray diffraction. Compound, lattice constant, variable coordinate  $x$  of 48f-site,  $R$ -factors ( $R_p$ ,  $R_{wp}$  and  $R_e$ ) and goodness of fit  $\chi^2$ .

Compound	$a$ (Å)	$x$ (48f)	$R_p$	$R_{wp}$	$R_e$	$\chi^2$
$\text{Ho}_2\text{Ti}_{1.9}\text{Mn}_{0.1}\text{O}_7$	10.0913(4)	0.329(1)	12.2	12.4	7.56	2.70
$\text{Dy}_2\text{Ti}_{1.9}\text{Mn}_{0.1}\text{O}_7$	10.0804(1)	0.327(1)	25.2	16.8	14.81	1.29

### **6.2.2.1 ac susceptibility of Ho<sub>2</sub>Ti<sub>1.9</sub>Mn<sub>0.1</sub>O<sub>7</sub> and Dy<sub>2</sub>Ti<sub>1.9</sub>Mn<sub>0.1</sub>O<sub>7</sub>**

To investigate this phenomenon, field dependent ac susceptibility of HTMO and DTMO has been measured. Figure 6.6 shows the temperature dependence of the real part of the ac susceptibility measured at 200 Hz for 0 T, 0.5 T and 0.75 T applied magnetic fields for both the compounds. It has been found that the spin ice freezing which does not appear without a magnetic field in HTO appears in HTMO even in absence of applied magnetic field (fig. 6.6 (a)). On application of an applied dc magnetic field, this freezing shows a shifting towards the higher temperature side. In case of DTMO,  $T_{ice}$  shifts towards higher temperature whereas  $T_f$  shifts towards the lower temperature side (see figure 6.6 (d)). On application of external magnetic field,  $T_{ice}$  freezing disappeared whereas  $T_f$  freezing shifted towards the higher temperature (figure 6.6 (e & f)). These observations suggest that altered magnetic interaction in HTMO and DTMO, spin freezing lies in the quantum critical region shifted towards the higher temperature whereas thermal classical spin freezing shifted towards the lower temperature. The appearance and shifting of spin freezing lie in the quantum critical region suggest alteration in energy barrier. Due to this alteration in energy barrier, a prominent change in the spin ice freezing takes place. This change in the spin ice freezing also follows the  $(x-x_C)^{1/2}$  variation further confirming the dominance of quantum fluctuation in these systems. The change in  $T_{ice}$  suggests that effect of altered effective energy barrier on the spin freezing closer to the quantum critical point is much significant due to  $(x-x_C)^{1/2}$  variation.



*Figure 6.6: Temperature dependence of the real part of ac susceptibility measured at the 200 Hz frequency for  $\text{Ho}_2\text{Ti}_2\text{O}_7$  and  $\text{Ho}_2\text{Ti}_{1.9}\text{Mn}_{0.1}\text{O}_7$  (a, b, & c) and for  $\text{Dy}_2\text{Ti}_2\text{O}_7$  and  $\text{Dy}_2\text{Ti}_{1.9}\text{Mn}_{0.1}\text{O}_7$  (d, e, & f) at different DC bias field.*

### 6.3 Conclusion

These results can be summarised as: in  $\text{Ho}_2\text{Ti}_2\text{O}_7$  both single ion spin freezing temperature ( $T_f$ ) and spin ice freezing temperature ( $T_{\text{ice}}$ ) lies in the quantum critical region whereas in  $\text{Dy}_2\text{Ti}_2\text{O}_7$  only  $T_{\text{ice}}$  lies in the quantum critical region. The obtained values of critical field at quantum critical point suggests higher effective energy barrier for spin relaxation in DTO in

comparison to HTO. The value of critical field represents magnitude of the magnetic field needed to influence spin freezing at absolute zero temperature. ac susceptibility study of B-site Mn substituted  $\text{Ho}_2\text{Ti}_{1.9}\text{Mn}_{0.1}\text{O}_7$  and  $\text{Dy}_2\text{Ti}_{1.9}\text{Mn}_{0.1}\text{O}_7$  shows that these substitutions affect  $T_{\text{ice}}$  freezing in more prominent way in comparison to the single ion freezing  $T_f$  in these compounds, which means that competing magnetic interactions acting in different temperature regime are one of the preliminary factors responsible for the alteration in quantum critical point in these compounds. This observed dependencies of the low temperature phases on non-thermal external variable, open a new route to investigate the underlying physics of geometrically frustrated magnetic materials in terms of quantum criticality at non-zero temperatures.